Nuclear Physics B176 (1980) 269–284

SINGLE π^+ PRODUCTION IN CHARGED CURRENT NEUTRINO-HYDROGEN INTERACTIONS

Aachen-Bonn-CERN-München-Oxford Collaboration

P. ALLEN, J. BLIETSCHAU, H. GRÄSSLER, D. LANSKE, R. SCHULTE and H.H. SEYFERT

III. Physikalisches Institut der Technischen Hochschule, Aachen, Germany

K. BÖCKMANN, P. CHECCHIA[1], C. GEICH-GIMBEL, H.G. HEILMANN, T. KOKOTT, B. NELLEN and R. PECH

Physikalisches Institut der Universität Bonn, Bonn, Germany

P. BOSETTI[2], V.T. COCCONI, B. CONFORTO[3], D.C. CUNDY, A. GRANT, D. HAIDT[4], P.O. HULTH, G. KELLNER, H. KLEIN, D.R.O. MORRISON, R. ORAVA[5], L. PAPE, P. SCHMID, W.G. SCOTT, H. WACHSMUTH and E. DE WOLF[6]

CERN, European Organization for Nuclear Research, Geneva, Switzerland

M. ADERHOLZ, N. SCHMITZ, R. SETTLES, K.L. WERNHARD and W. WITTEK

Max-Planck-Institut für Physik und Astrophysik, München, Germany

R. BATLEY, R. GILES, P. GROSSMANN, R. McGOW, G. MYATT, D.H. PERKINS, D. RADOJICIC, P. RENTON and B. SAITTA

University of Oxford, Department of Nuclear Physics, Oxford, UK

Received 23 June 1980
(Final version received 11 August 1980)

The reaction $\nu p \to \mu^- p \pi^+$ (777 events) is studied at neutrino energies from 5 to 200 GeV. A total of 551 events fit the channel $\nu p \to \mu^- \Delta^{++}(1232)$ with χ^2 probability greater than 2%. Decay angular distributions of the Δ^{++} are investigated and the density matrix elements are studied as functions of Q^2, the square four-momentum transfer. The total Δ^{++} production cross section and the differential cross section $d\sigma/dQ^2$ are determined. Using the Schreiner-von Hippel parametrization of the Adler model, the value of the axial mass determined by fitting the total

[1] Now at Università di Padova, Istituto di Fisica, Padova, Italy.
[2] CERN Fellow from III. Physikalisches Institut, Aachen, Germany.
[3] Now at Università di Firenze, Istituto di Fisica, Firenze, Italy.
[4] Now at DESY, Hamburg, Germany.
[5] Now at FNAL, Batavia, Illinois, USA.
[6] Now at NIKHEF-H, Amsterdam, Netherlands.

cross sections above 20 GeV is $M_A = 0.85 \pm 0.10$ GeV. The model describes the differential cross sections reasonably well above $Q^2 \simeq 0.2$ GeV^2. Disagreements, however, are found for some values of the density matrix elements of the Δ^{++} decay angular distributions and their Q^2 dependence. The $(p\pi^+)$ mass region above the $\Delta^{++}(1232)$ contains evidence for the presence of higher mass Δ^{++} resonances and, above 2 GeV, for the forward emission of fast π^+.

1. Introduction

The reaction

$$\nu p \rightarrow \mu^- p \pi^+ \tag{1}$$

is the simplest neutrino interaction to identify experimentally in a hydrogen bubble chamber, as all three final-state particles are charged. However, the results so far available derive from experiments either at low energies or of low statistics.

Reaction (1) was studied at the CERN PS with the 1.2 m heavy liquid bubble chamber [1] and with Gargamelle [2], both chambers filled with propane, and at the Argonne ZGS with the 12′ bubble chamber filled with hydrogen and deuterium [3]. In all of these experiments the neutrino energy was smaller than 10 GeV. At higher energies, the only information available derives from an experiment at FNAL [4] with the 15′ bubble chamber filled with hydrogen (200 events).

The work described in this paper is based on 777 events which fit reaction (1) with a χ^2 probability larger than 2%, produced by neutrinos with energies from 5 to 200 GeV.

Of these events, 551 belong to the subchannel

$$\nu p \rightarrow \mu^- \Delta^{++}(1232), \tag{2}$$

with the effective mass of the $(p\pi^+)$ system smaller than 1.4 GeV.

Total and differential cross sections for Δ^{++} production are determined, as well as the Δ^{++} angular distributions. This larger sample of events also allows a study of the density matrix elements as functions of the squared four-momentum transfer, Q^2.

Preliminary results based on a subset of the final sample have been reported [5].

The theoretical models which have been proposed to describe single pion production by neutrinos fall essentially into three categories [6]:

(a) Isobar models in which it is assumed that the final state is dominated by the production of a $(p\pi^+)$ resonance which is treated as an elementary particle [7–9].

(b) Dynamical calculations mostly based on dispersion relations [10–14].

(c) Relativistic harmonic oscillator quark models [15, 16] whose predictions are very similar to those of type (b), in particular to those of the Adler model [13].

Comparisons of the results of previous experiments with these different calculations [2–4] have so far favoured the Adler model as the most successful description of the physical situation.

This paper is organized as follows: in sect. 2 the experimental data for the reaction $\nu p \to \mu^- p\pi^+$ are presented. In sect. 3 the channel $\nu p \to \mu^- \Delta^{++}(1232)$ is studied. A comparison with a parametrization of the Adler model is presented in sect. 4 and the value of the axial mass M_A is determined. The high-mass region of the $(p\pi^+)$ spectrum is discussed in sect. 5.

2. The data

Approximately 285 000 photographs were taken of the BEBC bubble chamber filled with hydrogen, exposed to the wideband neutrino beam at the CERN SPS. This exposure corresponds to $\sim 10^{18}$ protons on the SPS target at 350 GeV.

The film was scanned for neutral induced events with three or more prongs and visible energy greater than ~ 1.5 GeV. The events were measured on film-plane digitizers and reconstructed using the HYDRA programming chain. The muons were identified by a two-plane external muon identifier (EMI) whose efficiency is $\sim 98\%$ for $p_\mu > 10$ GeV/c. The events were accepted if they were within a fiducial volume of 19 m^3 (corresponding to $> 1.1\ t$ of H_2) and if the energy of the neutrino E_ν was larger than 5 GeV.

A total of 8108 charged current (CC) events was obtained with energies from 5 to 200 GeV. Of these, $\sim 10\%$, i.e., 819 events gave a fit to reaction (1), $\nu p \to \mu^- p\pi^+$, with the fitted neutrino energy greater than 5 GeV, and with χ^2 probability greater than 0.01%.

Table 1 reports the number of CC events with a single μ^- identified either by the EMI or by the fit and the number of events that fit reactions (1) and (2).

Fig. 1 shows the χ^2 probability distributions of the 819 and 576 events which fit reactions (1) and (2), respectively. The accumulation of events towards the smallest fit probabilities was investigated and found to contain contamination by events in which unseen neutral particles are also produced. Consequently, in the following analysis only the events with $P(\chi^2) > 2\%$ have been used, i.e., 777 events of reaction (1) and 551 events of reaction (2).

The particles in the final state of reaction (1) were fitted unambiguously in $\sim 87\%$ of the events. Among the non-uniquely identified events, we have found

TABLE 1
Number of (a) charged current (CC) events, (b) events fitting the reaction $\nu p \to \mu^- p\pi^+$ and (c) fitting the reaction $\nu p \to \mu^- \Delta^{++}(1232)$

μ^- identification	(a) CC events	(b) $\nu p \to \mu^- p\pi^+$ all	(b) $P(\chi^2) > 2\%$	(c) $\nu p \to \mu^- \Delta^{++}$ all	(c) $P(\chi^2) > 2\%$
by EMI	7747	772	733	549	527
by fit only	361	47	44	27	24
total	8108	819	777	576	551

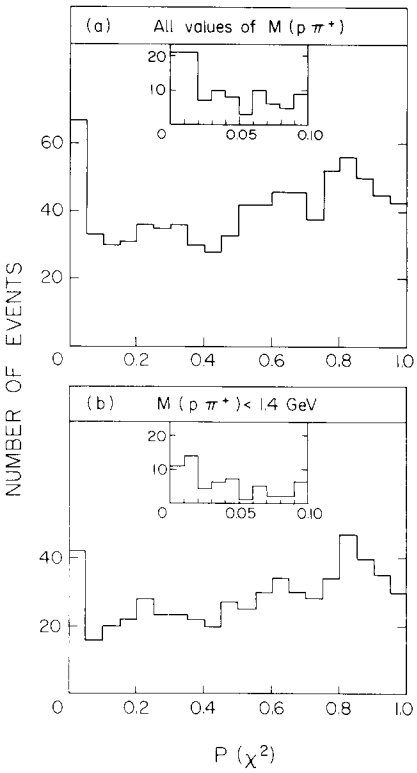

Fig. 1. χ^2 probability distributions for the (a) 819 events fitting the reaction $\nu p \to \mu^- p\pi^+$ and (b) 576 events fitting the reaction $\nu p \to \mu^- \Delta^{++}(1232)$. The insets show in detail the distributions up to $P(\chi^2) = 0.10$.

that several types of ambiguity occur. These are:

(a) K^+/π^+ or

(b) p/π^+ ambiguity for the positive secondary tracks;

(c) K^0/ν ambiguity for the incident track;

(d) combinations of (a), (b) and (c).

The relative frequency of the four types is 3 : 3 : 5 : 2. It should be mentioned that most of the events where there is a p/π^+ or K^0/ν ambiguity belong to reaction (2). The opposite is true of the other cases. For the non-uniquely identified events, we have accepted the fit with the highest probability.

3. Study of the $\Delta^{++}(1232)$

3.1. THE INVARIANT-MASS SPECTRUM

The $(p\pi^+)$ mass distribution for the 777 events of reaction (1) used in the analysis is shown in fig. 2. The $\Delta^{++}(1232)$ peak is clearly dominant.

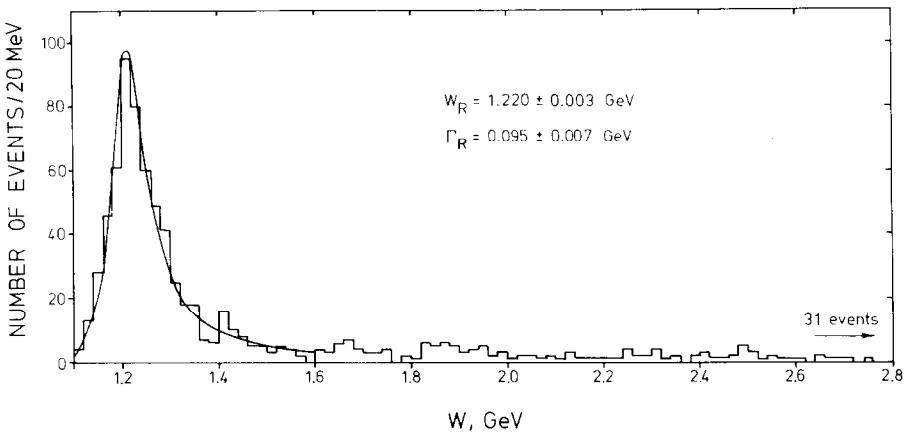

Fig. 2. ($p\pi^+$) effective-mass distribution for the 777 events fitting the reaction $\nu p \to \mu^- p\pi^+$ with χ^2 probability greater than 2%. The solid line is the result of a fit using a relativistic Breit-Wigner function with Γ energy dependence of form (d). The fitted values of the Δ^{++} parameters M_R and Γ_R are indicated.

To obtain the best values for the resonance mass and width several fits have been performed with a relativistic Breit-Wigner function of the form

$$f(W) = \frac{W_R \Gamma / \pi}{(W^2 - W_R^2)^2 + W_R^2 \Gamma^2} \tag{3}$$

plus a non-resonant background. In eq. (3), W is the invariant mass of the ($p\pi^+$) system, W_R is the value of W at resonance and Γ is the resonance width. Several forms of energy dependence of Γ have been considered:

(a) $\Gamma = \Gamma_R$, where Γ_R is the energy independent width at resonance.

(b) $\Gamma = \Gamma_R(p/p_R)$ (s-wave dependence), where p is the momentum of the π^+ or proton in the resonance rest system, and p_R is the same quantity at resonance.

(c) $\Gamma = \Gamma_R(p/p_R)^3$ (p-wave dependence).

(d) $\Gamma = \Gamma_R(p/p_R)^3 (p_R^2 + x^2)/(p^2 + x^2)$ with $x = 0.16$. This is the form used by Walker [17] in his analysis of Δ resonances in photoproduction.

Fits have been performed over the range $W = 1.1 - 1.6$ GeV (609 events). The energy-independent width of case (a) and the p-wave dependence of case (c) both gave unacceptable χ^2/NDF values. The fits corresponding to cases (b) and (d) gave practically identical values for W_R and Γ_R. The result of the fit with the parametrization of case (d) is the solid curve in fig. 2.

The parameters of the $\Delta^{++}(1232)$ are found to be

$$W_R = 1.220 \pm 0.003 \text{ GeV},$$

$$\Gamma_R = 0.095 \pm 0.007 \text{ GeV}. \tag{4}$$

The fitted background is $\sim 14\%$ in the mass range 1.4 to 1.6 GeV. Below 1.4 GeV, however, the background is consistent with zero and so we consider all 551 events as belonging to the reaction $\nu p \to \mu^- \Delta^{++}(1232)$.

3.2. DECAY ANGULAR DISTRIBUTION OF THE $\Delta^{++}(1232)$

Fig. 3 shows the angular distributions of the π^+ in the Δ^{++} c.m.s. for all events. The azimuthal and polar decay angles ϕ and θ, respectively, are defined in a right-handed coordinate system, in which the z axis is along the momentum transfer direction $\boldsymbol{q} = \boldsymbol{p}_\nu - \boldsymbol{p}_\mu$ and the y axis along the normal to the production plane $\boldsymbol{p}_\nu \times \boldsymbol{p}_\mu$ (fig. 4). The distribution shows a slight excess of events with a forward π^+. The asymmetry parameter is $A = (N_F - F_B)/(N_F + N_B) = 0.06 \pm 0.04$.

Assuming time-reversal invariance in the production process of the Δ^{++}, the angular distributions are described by

$$\frac{d\sigma}{d\Omega} = \frac{\sigma}{\sqrt{4\pi}} \left[Y_0^0 - \frac{2}{\sqrt{5}} \left(\hat{\rho}_{33} - \tfrac{1}{2} \right) Y_2^0 + \frac{4}{\sqrt{10}} \hat{\rho}_{31} \operatorname{Re} Y_2^1 - \frac{4}{\sqrt{10}} \hat{\rho}_{3-1} \operatorname{Re} Y_2^2 \right], \quad (5)$$

for the weak production of a pure Δ^{++} state of spin $\frac{3}{2}$. The functions Y_l^m are the spherical harmonics and the $\hat{\rho}_{ij}$, the density matrix elements for weak production,

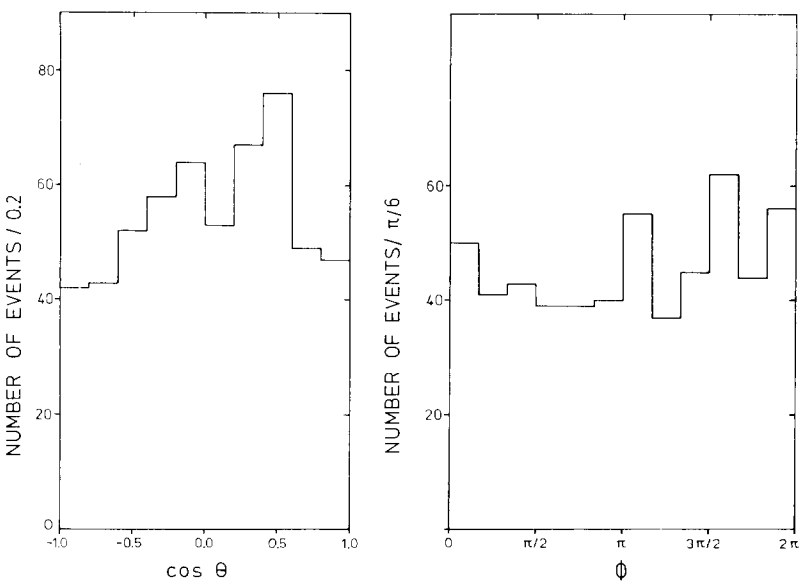

Fig. 3. Δ^{++} decay angular distributions. The angles θ and ϕ are the polar and azimuthal angles of the π^+ in the Δ^{++} c.m.s., defined as in fig. 4.

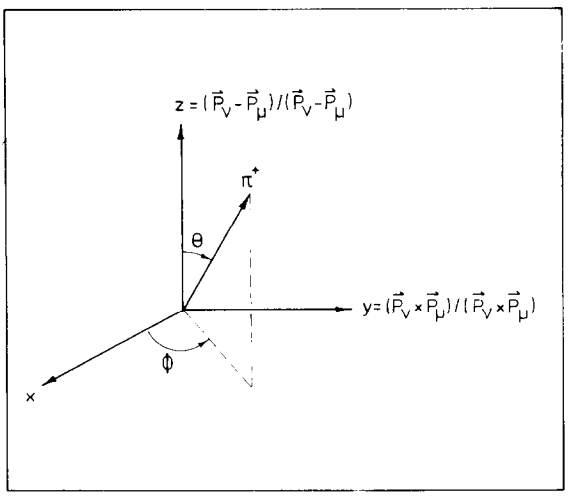

Fig. 4. Definition of the π^+ polar (θ) and azimuthal (ϕ) angles in the c.m.s. of the decaying Δ^{++}.

are defined by

$$\hat{\rho}_{33} = \tfrac{1}{2} + \tfrac{1}{2}\left[\rho_{33} + \rho_{-3-3} - \rho_{11} - \rho_{-1-1}\right],$$

$$\hat{\rho}_{31} = \rho_{31} - \rho_{-1-3},$$

$$\hat{\rho}_{3-1} = \rho_{3-1} + \rho_{1-3}. \tag{6}$$

The experimental values of the average density matrix elements, $\hat{\rho}_{ij}$, calculated in three different regions of Q^2, using the method of moments, are given in table 2.

TABLE 2
Comparison of the Δ^{++} density matrix elements with theoretical predictions

Q^2 (GeV)^2		0 – 0.25	0.25 – 0.5	0.5 – 3.0
$\langle\hat{\rho}_{33}\rangle$	exp.	0.60 ± 0.08	0.70 ± 0.09	0.70 ± 0.07
	model	0.48	0.70	0.74
$\langle\hat{\rho}_{31}\rangle$	exp.	− 0.13 ± 0.04	− 0.01 ± 0.05	0.04 ± 0.04
	model	− 0.29	− 0.14	− 0.04
$\langle\hat{\rho}_{3-1}\rangle$	exp.	− 0.05 ± 0.04	− 0.12 ± 0.05	0.04 ± 0.04
	model	− 0.06	0.08	0.26

3.3. CROSS SECTION FOR $\Delta^{++}(1232)$ PRODUCTION

In order to calculate the total cross section for reaction (2) the neutrino flux was determined using the measured muon yields and recent pion and kaon production data. The muon fluxes were measured in the first five gaps in the shielding downstream in the neutrino beam over a circle of radius 37.5 cm around the beam axis. The π and K fluxes were determined from the predictions of the thermodynamic model [18] adjusted to the results on π and K production rates in a 400 GeV pBe experiment [19]. The neutrino flux obtained is reliable to within 8% for events with an incoming neutrino energy above 20 GeV.

The Δ^{++} production cross sections are thus calculated using this neutrino flux for events which have an incoming energy above 20 GeV. For the events of lower energies the cross section was obtained from the total number of CC events using the average CC cross section

$$\sigma_{\nu p \to CC} = (0.433 \pm 0.033) \cdot 10^{-38} \cdot E \cdot \mathrm{cm}^2 .$$

The energy of each CC event was determined by correcting the measured energy for the energy missed in neutral particles, using a transverse momentum balance method [20]. Finally, the number of Δ^{++} events was corrected for the loss (~ 10 events) due to the cut at 2% in the fit probability, for an estimated 2% loss of events at small values of Q^2, and a 1% scanning loss.

In table 3 are given the values of the Δ^{++} production cross section for events with $W < 1.4$ GeV measured in various energy intervals. The errors quoted are statistical. It is important to remember that the points for $E_\nu < 20$ GeV suffer from large systematic errors and depend on the knowledge of the CC inclusive cross section. On the contrary, the points above 20 GeV, based on direct knowledge of the neutrino flux, provide the first absolute determinations for the Δ^{++} cross sections at high energy and have a systematic error of only 8%.

The cross section for reaction (2) fitted over the neutrino energy from 20 to 200 GeV is $(0.49 \pm 0.05) \cdot 10^{-38}$ cm^2. The error given here includes the uncertainty in

TABLE 3
Δ^{++} production cross sections ($W < 1.4$ GeV) in various intervals of the neutrino energy E_ν

E_ν (GeV)	$\sigma(10^{-38} \cdot \mathrm{cm}^2)$
5–10	0.60 ± 0.06
10–15	0.53 ± 0.05
15–20	0.62 ± 0.06
20–30	0.52 ± 0.05
30–50	0.51 ± 0.07
50–100	0.39 ± 0.08
> 100	0.44 ± 0.20

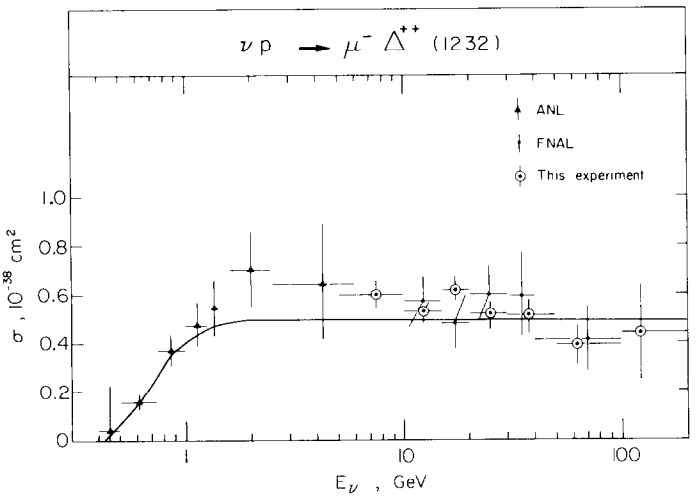

Fig. 5. Production cross section for the reaction $\nu p \to \mu^- \Delta^{++}$ as a function of the neutrino energy, E_ν. The results of this experiment (double circles) are plotted together with those of the ANL (solid triangles) and FNAL (solid circles) experiments of refs. [3, 4]. The solid line is the prediction of the parametrization of the Adler model described in the text, with the value $M_A = 0.85$ GeV for the axial mass.

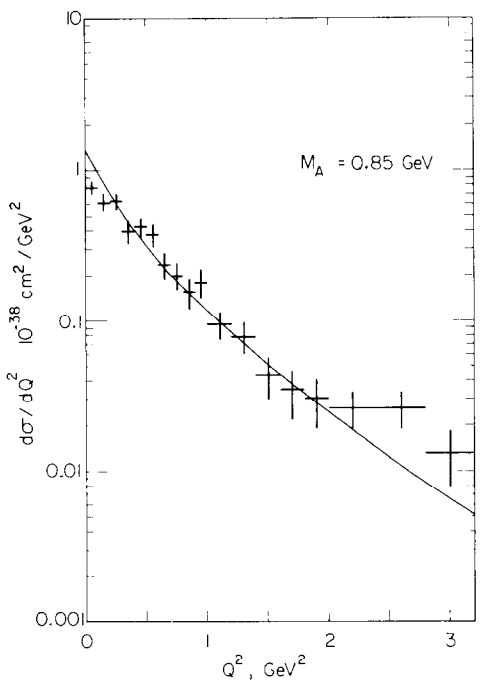

Fig. 6. Differential cross section $d\sigma/dQ^2$ for the reaction $\nu p \to \mu^- \Delta^{++}$. The solid line is the prediction of the Adler model with the parametrization described in the text, and with the value $M_A = 0.85$ GeV for the axial mass.

the flux. In order to correct for Δ^{++} events with $W > 1.4$ GeV we have integrated the Breit-Wigner expression (3) with the stated best fit parameters of form (d) in subsect. 3.1, up to $W = 3$ GeV. This gives a correction factor of $\sim 20\%$ and leads to a cross section for total Δ^{++} production of $(0.59 \pm 0.06) \cdot 10^{-38}$ cm^2.

In fig. 5 our results, uncorrected for the high-mass tail of the Δ^{++} are shown together with those from other experiments [3, 4]. The agreement among the various experiments is satisfactory. Though our points above 20 GeV are consistent with a Δ^{++} cross section independent of energy, the general trend of all the data available seems to suggest a slight decrease of the Δ^{++} cross section from ~ 2 to 200 GeV.

The differential cross section $d\sigma/dQ^2$ for the events of reaction (2) is shown in fig. 6. The 2% loss at small values of Q^2 has been corrected for by adding 7 events to the first bin, and 4 to the second one. The distribution has been normalized to the experimental cross section of $0.49 \cdot 10^{-38}$ cm^2.

4. Comparison with theoretical predictions

Among the various theoretical models for the reaction $\nu p \to \mu^- \Delta^{++}$ [7–16], we have chosen to compare our results with the predictions of the Schreiner and von Hippel parametrization [21] of the Adler model [13], which has been reasonably successful in describing the results of previous experiments [2–4].

Following Schreiner and von Hippel [21], the differential cross section for reaction (2) is given by

$$\frac{d^2\sigma}{dQ^2\, dW^2} = \frac{G}{16\pi M^2}\left[K_1 \hat{W}_1 + K_2 \hat{W}_2 + K_3 \hat{W}_3 \right], \tag{7}$$

where $Q^2 = -q^2 = -(p_\nu - p_\mu)^2$, $G \simeq 0.99 \cdot 10^{-5}\ M^{-2}$ is the Fermi constant and M is the proton mass. The kinematic factors K_1, K_2 and K_3, beside depending on W and Q^2, contain the dependence of the cross section on the incident neutrino energy. W_1, W_2 and W_3 are structure functions depending only on Q^2 and W and are quadratic functions of the matrix elements of the hadronic weak current. These matrix elements can be expressed in terms of a Breit-Wigner function and a sum of Rarita-Schwinger form factors which contain the Q^2 dependence. The vector form factors are taken to be

$$|C_3^V(Q^2)|^2 = (2.05)^2\left[1 + 9(Q^2)^{1/2} \right] \exp\left[-6.3(Q^2)^{1/2} \right],$$

$$C_4^V(Q^2) = -\frac{M}{W} C_3^V(Q^2),$$

$$C_5^V(Q^2) = 0,$$

$$C_6^V(Q^2) = 0,$$

and the axial vector form factors

$$C_i^A(Q^2) = C_i^A(0)\frac{1 + aQ^2/(b+Q^2)}{(1+Q^2/M_A^2)^2}, \qquad i = 3-5,$$

$$C_6^A(Q^2) = \frac{-g_\Delta f_\pi M}{2\sqrt{3}\,(m_\pi^2+Q^2)}\,\frac{1}{(1+Q^2/M_A^2)^2},$$

with $C_3^A(0) = 0$, $C_4^A(0) = -0.3$, $C_5^A(0) = 1.2$ and $a = -1.2$, $b = 2.0$. The parameter $g_\Delta = 28.6$ is the $\Delta^{++}\to p\pi^+$ coupling constant and $f_\pi = 0.97\ m_\pi$ is the pion decay constant.

For the Breit-Wigner function, the form used in ref. [21] is the non-relativistic s-wave distribution, with $W_R = 1.232$ GeV and $\Gamma_R = 0.120$ GeV.

The only free parameter of the model is the axial mass, M_A, which is to be determined by the experiment.

A fit to the total cross sections of table 3 over the energy range from 20 to 200 GeV gives

$$M_A = 0.85 \pm 0.10\ \text{GeV}. \tag{8}$$

The error on this value corresponds to the upper and lower bounds on the cross section*. Our result is to be compared with the value $M_A = 0.93 \pm 0.11$ GeV obtained in the ANL experiment [3] at lower energies and with the FNAL result at energies similar to ours, $M_A = 1.15 \pm 0.10$ GeV [4], both of which, however, were determined with a somewhat different procedure. The curve calculated with our value of M_A (solid line in fig. 5) is a moderately satisfactory fit to the data below 20 GeV. The model would not describe a Δ^{++} cross section decreasing with increasing energy above ~ 2 GeV.

The total cross section data are more sensitive to the value of M_A than those of the differential cross section. In the Q^2 range used, the shape of the differential cross section is in fact determined by the vector contributions much more than by the axial ones, these latter becoming important only at $Q^2 < 0.4$ GeV^2 (fig. 7). The value $M_A = 0.85$ GeV has therefore been used to calculate the curve drawn in fig. 6. The model predictions describe well the experimental results for $Q^2 > 0.2$ GeV ($\chi^2 \approx 1$), but predict more events than observed at lower Q^2 values ($\chi^2 = 15$ and 6 in the first and second bin, respectively).

* If instead of the s-wave non-relativistic form of the Breit-Wigner width we use the forms (b) and (d) of subsect. 3.1, with the best fit parameters of eq. (4) derived from our mass spectrum, the values of M_A obtained from fitting the experimental cross section are 0.70 ± 0.10 and 0.79 ± 0.10 GeV, respectively.

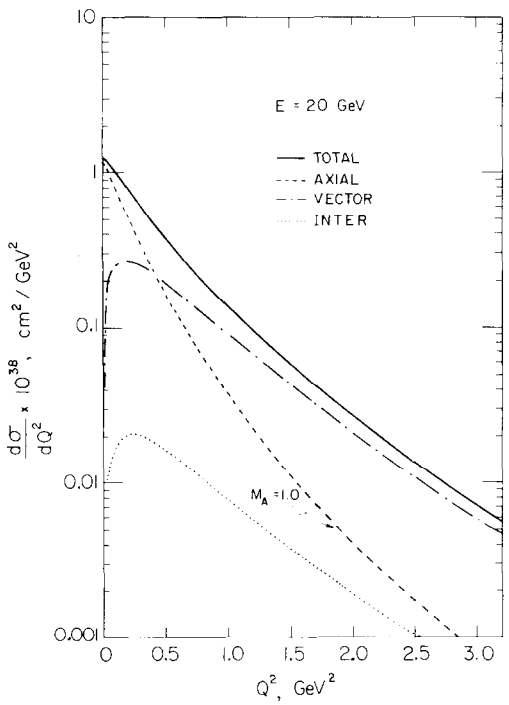

Fig. 7. Vector and axial contributions to the differential cross section $d\sigma/dQ^2$ as functions of Q^2, calculated at $E_\nu = 20$ GeV.

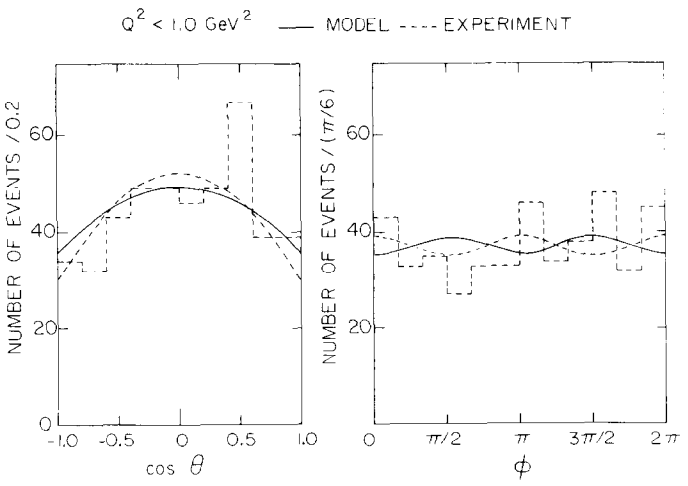

Fig. 8. Comparison of the experimental decay angular distributions for $Q^2 < 1$ GeV^2 with the predictions of the model, $\hat{\rho}_{33} = 0.597$ and $\hat{\rho}_{3-1} = 0.041$ (solid line). The dashed line is calculated from the experimental values of $\hat{\rho}_{33} = 0.662$ and $\hat{\rho}_{3-1} = -0.046$.

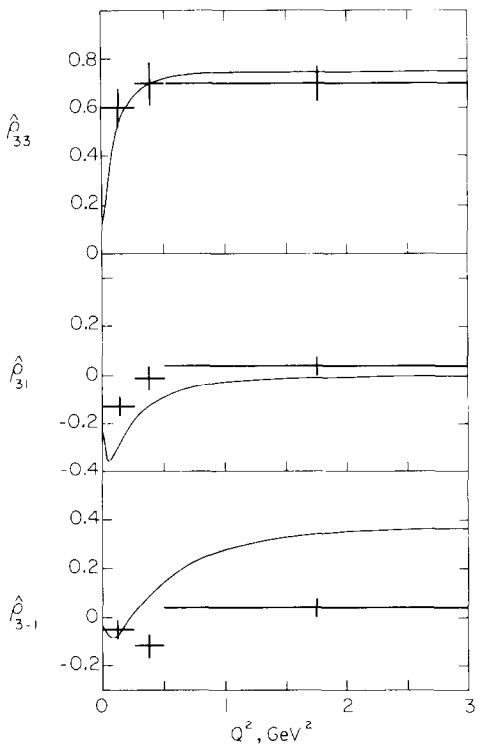

Fig. 9. Comparison of experimental results and model predictions (solid lines) for the Q^2 dependence of the density matrix elements $\hat{\rho}_{33}$, $\hat{\rho}_{31}$ and $\hat{\rho}_{3-1}$ of the Δ^{++} decay.

The prediction of the model for the decay angular distribution is compared with the experimental results (for $Q^2 < 1$ GeV^2) in fig. 8. No asymmetry is predicted by the simplified version of the Adler model used. The experimental value of the asymmetry parameter is $A = 0.07 \pm 0.05$.

The solid lines in fig. 9 are the model prediction for the Q^2 dependence of the density matrix elements, again calculated with $M_A = 0.85$ GeV. These predictions are very similar to those from the quark model of Andreadis et al. [15] and of Ravndal [16]. The predicted values of $\langle \hat{\rho}_{ij} \rangle$ are compared with the experimental results also in table 2. From that table and from fig. 9 one can see that, while agreement is found for $\hat{\rho}_{33}$, the predicted values of $\hat{\rho}_{31}$ are consistently more negative than the measured ones. Furthermore, the measured values of $\hat{\rho}_{3-1}$ do not have the Q^2 dependence predicted by the model.

5. The higher ($p\pi^+$) mass region

Fig. 10 shows the two-dimensional plot of the ($p\pi^+$) mass, W, versus $\cos\theta$, where θ is the π^+ emission angle in the rest frame of the hadrons for the events of

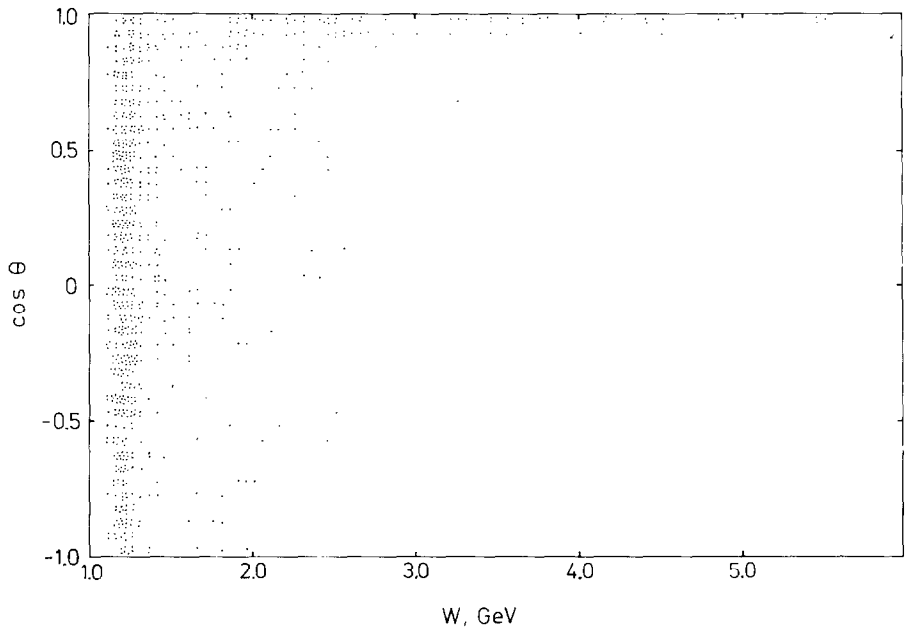

Fig. 10. The invariant mass of the $p\pi^+$ system, W, versus $\cos\theta$, the emission angle of the π^+ in the hadron rest frame.

reaction (1) with $E > 5$ GeV and $P(\chi^2) > 2\%$. The Δ^{++} band is clearly seen. The plot also shows the presence of backward emitted π^+'s, up to $(p\pi^+)$ masses of ~ 2.5 GeV, which can be taken as evidence for the production of heavier Δ^{++} resonances.

The quark model of ref. [15] predicts cross sections of $\sim 0.1 \cdot 10^{-38}$ cm^2 for Δ^{++} resonances in the region 1650–1690 MeV [$S_{31}(1650)$, $D_{33}(1670)$ and $P_{33}(1690)$] and of $\sim 0.08 \cdot 10^{-38}$ cm^2 for the region 1890–1960 MeV [$F_{35}(1890)$, $P_{31}(1910)$, $F_{37}(1950)$, $D_{35}(1960)$]. In our sample, we find 36 events with $1.6 \leqslant W \leqslant 1.8$ GeV and 38 events with $1.8 \leqslant W \leqslant 2$ GeV. This is compatible with the cross sections predicted by the quark model, if one assumes that the branching ratio for the $(p\pi^+)$ decay channel is $\sim 30\%$.

Approximately 10% of the total events have $W > 2$ GeV. They are characterized by the forward emission of a fast π^+, which is indicative of one-pion exchange mechanisms. The average cross section for such events is $\sim 0.1 \cdot 10^{-38}$ cm^2.

6. Conclusions

Reaction (1) has been studied (777 events) for neutrino energies between 5 and 200 GeV. The dominant subchannel, with 551 events, is $\nu p \to \mu^- \Delta^{++}(1232)$. Values for its production cross section for $E_\nu = 5$–20 GeV have been obtained by normalizing to the corresponding numbers of CC events. From 20 to 200 GeV, absolute

values of the cross section could be determined, based on the direct knowledge of the neutrino flux, and their average is $(0.59 \pm 0.06) \cdot 10^{-38}$ cm^2.

Our experimental points are in agreement with the results of other experiments. The trend of all points available suggests that the Δ^{++} production cross section may decrease slightly with increasing neutrino energy from $\sim$2 to 200 GeV.

The differential cross section $d\sigma/dQ^2$, the Δ^{++} decay angular distributions and the density matrix elements $\hat{\rho}_{ij}$ have been determined.

The energy dependence of the $\Delta^{++}(1232)$ total production cross section is approximately described by the Schreiner-von Hippel parametrization of the Adler model with the value $M_A = 0.85 \pm 0.10$ GeV for the axial mass determined by using our total cross section above 20 GeV. However, the differential cross section $d\sigma/dQ^2$ shows some disagreement with the model for $Q^2 < 0.2$ GeV^2. Disagreements with experiment are also found in the predictions of the model for some of the values of the density matrix elements and their Q^2 dependence.

Indication is seen for the presence, above the $\Delta^{++}(1232)$, of higher mass Δ^{++} resonances at the level predicted by the quark model. The $(p\pi^+)$ mass region above 2 GeV is characterized by the forward emission of a fast π^+, probably due to one-pion exchange mechanisms.

We would like to thank the scanning, measuring and computing teams in our laboratories and the CERN staff for the operation of the SPS accelerator, the BEBC bubble chamber and associated equipment. The Aachen Group is pleased to acknowledge helpful discussions with Dr. D. Rein.

References

[1] I. Budagov et al., Phys. Lett. 29B (1969) 524
[2] W. Lerche et al., Phys. Lett. 78B (1978) 510
[3] J. Campbell et al., Phys. Rev. Lett. 30 (1973) 335;
S.J. Barish et al., Phys. Rev. D19 (1979) 2521
[4] J. Bell et al., Phys. Rev. Lett. 41 (1978) 1008; 1012
[5] P. Schmid, Neutrinos '78, ed., E.C. Fowler, Purdue (1978) 939;
B. Conforto, Proc. Topical Conf. on Neutrinos at accelerators;
Ed., A.G. Michette, P.B. Renton, Oxford (1978) 90 and Neutrino 79;
Ed., A. Haatuft and C. Jarlskog, Bergen (1979) vol. 2, p. 515
[6] C.H. Llewellyn-Smith, Phys. Reports 3 (1972) 261
[7] S.M. Berman and M. Veltmann, Nuovo Cim. 38 (1965) 993
[8] C.H. Albright and L.S. Liu, Phys. Rev. Lett. 13 (1964) 673; 14 (1964) 324; Phys. Rev. 140B (1965) 748
[9] C.W. Kim, Nuovo Cim. 37 (1965) 142
[10] Ph. Salin, Nuovo Cim. 48A (1967) 506
[11] J. Bijtebier, Nucl. Phys. B21 (1970) 158
[12] P.A. Zucker, Phys. Rev. D4 (1971) 3350
[13] S.L. Adler, Ann. of Phys. 50 (1968) 189; Phys. Rev. D12 (1975) 2644
[14] G.L. Fogli and G. Nardulli, Nucl. Phys. B160 (1979) 116
[15] P. Andreadis et al., Ann. of Phys. 88 (1974) 242 (E:97 (1976) 576)
[16] F. Ravndal, Nuovo Cim. Lett. 3 (1972) 631; Nuovo Cim. 18A (1973) 385

[17] R.L. Walker, Phys. Rev. 182 (1969) 1729
[18] R. Hagedorn and J. Ranft, Nucl. Phys. B48 (1972) 157;
Computer Program SPUKJ, CERN Computer Library.
[19] H. Atherton et al., CERN Yellow Report, to be published
[20] G. Myatt, ECFA 300 Working Group Report, CERN/ECFA 72-4, vol. 2, p. 117
[21] P.A. Schreiner and F. von Hippel, Phys. Rev. Lett. 30 (1973) 339; Nucl. Phys. B58 (1973) 333